



Published in final edited form as:

*Bioorg Med Chem Lett.* 2010 March 1; 20(5): 1767–1770. doi:10.1016/j.bmcl.2010.01.036.

## Development of Improved Inhibitors of Wall Teichoic Acid Biosynthesis with Potent Activity Against *Staphylococcus aureus*

Kyungae Lee<sup>a</sup>, Jennifer Campbell<sup>b</sup>, Jonathan G. Swoboda<sup>b</sup>, Gregory D. Cuny<sup>c</sup>, and Suzanne Walker<sup>b,\*</sup>

<sup>a</sup> The New England Regional Center of Excellence in Biodefense and Emerging Infectious Diseases (NERCE/BEID), Harvard Medical School, Boston, MA 02115, USA

<sup>b</sup> Department of Microbiology and Molecular Genetics, Harvard Medical School, Boston, MA 02115, USA

<sup>c</sup> Laboratory for Drug Discovery in Neurodegeneration, Brigham & Women's Hospital and Harvard Medical School, Cambridge, MA 02139, USA

### Abstract

A small molecule (**1835F03**) that inhibits *Staphylococcus aureus* wall teichoic acid biosynthesis, a proposed antibiotic target, has been discovered. Rapid, parallel, solution-phase synthesis was employed to generate a focused library of analogs, providing detailed information about structure-activity relationships and leading to the identification of targocil, a potent antibiotic.

### Keywords

Wall teichoic acids (WTAs); *Staphylococcus aureus*; antibiotic; bacteriostatic; structure-activity relationship (SAR); triazoloquinazoline; targocil

More people now die from hospital-acquired methicillin-resistant *S. aureus* infections in the United States than from HIV/AIDs.<sup>1</sup> Until recently, vancomycin was known as the “last line of defense” against these infections, but high-level vancomycin resistance has now begun to appear in *S. aureus*.<sup>2–4</sup> Although two new classes of antibiotics to treat *S. aureus* infections have been introduced in the past decade, clinical resistance to each has already appeared and can be expected to spread.<sup>5–7</sup> For these reasons, a deep pipeline of novel antibiotics is required to combat MRSA infections.<sup>8</sup>

One suggested but as yet unexploited antibiotic target in *S. aureus* is wall teichoic acid (WTA) biosynthesis.<sup>9</sup> 10 WTAs are anionic, phosphate-rich, carbohydrate-based polymers that are synthesized on a lipid carrier inside the bacterial cell before being transported to the cell surface where they are covalently linked to peptidoglycan.<sup>11</sup> Their biological functions are diverse, ranging from cation homeostasis to critical roles in host colonization.<sup>12</sup> They are proposed virulence factors since deleting the biosynthetic pathway by knocking out the first gene (*tarO*) prevents infection. The downstream enzymes in the this pathway are potential antibiotic

\*To whom correspondence should be addressed: 200 Longwood Avenue, Boston, MA 02115; Tel: 617-432-5488; Suzanne\_Walker@hms.harvard.edu.

**Publisher's Disclaimer:** This is a PDF file of an unedited manuscript that has been accepted for publication. As a service to our customers we are providing this early version of the manuscript. The manuscript will undergo copyediting, typesetting, and review of the resulting proof before it is published in its final citable form. Please note that during the production process errors may be discovered which could affect the content, and all legal disclaimers that apply to the journal pertain.

targets since initiating flux into the biosynthetic pathway without completing it is deleterious to bacterial viability.<sup>13</sup>

We have discovered the first small molecule that specifically inhibits WTA biosynthesis using a cell-based, pathway-specific high-throughput screen that reports only on the antibiotic targets in the pathway. From a screen of 55,000 compounds, we identified **1835F03** (**1**) as a WTA-active antibiotic.<sup>14</sup> Compound **1** has good antibiotic activity (low  $\mu\text{M}$ ) against all *S. aureus* strains tested, including both hospital- and community-acquired MRSA isolates. We identified the target of **1** as TarG, the transmembrane component of the two component ABC transporter that exports WTAs from the cytoplasm to the external surface of the bacterial membrane where they are attached to peptidoglycan (Figure 1).<sup>14</sup> Two other compounds (**1856A19** and **1856K21**) that share a similar core with **1** were also identified as confirmed “hits” from the screen, but their potencies were lower (Figure 2). Moreover, commercial analogs of this class of inhibitors (**1856A19** and **1856K21**) appeared to have diminished target specificity relative to **1** since they showed partial growth inhibitory activity against the  $\Delta\text{tarO}$  mutant strain (see Supplementary Table 1). Therefore we focused on **1** as a lead for optimization.

The commercially available analogs of compound **1** had limited structural variations and all lacked activity (see Supplementary Figures 1 and 2). Therefore, we prepared a focused library of compound **1** analogs in order to identify sites on the scaffold that could be altered to improve potency without sacrificing selectivity for the target. The studies reported below provide key information about where this class of compounds is amenable to modification and have led to the identification of an analog that is ten times more potent than **1** and is non-toxic in mice at doses of 75 mg/kg.

Based on the structure of **1** (**1835F03**), libraries of compounds with varying core substitution and side chains were prepared. The triazoloquinazoline core was synthesized following previously published methods (Scheme 1).<sup>15</sup> The 2-azidobenzoic acid or ester, prepared from the corresponding anthranilic acid derivative, was heated with an arylsulfonylacetonitrile in the presence of base to furnish the triazoloquinazolone framework in one step. This reaction is believed to proceed *via* 1,3-dipolar cycloaddition of the azide to the enolate form of the nitrile, followed by cyclocondensation of the resulting aminotriazole. The yields of the triazoloquinazolones varied depending on the substituents on the azidobenzoic acid. While the cyclization proceeded smoothly with electron-deficient ring systems, such as chloro- or nitro-substituted azidobenzoic acids, yields were low to moderate with electron-rich substrates.

However, use of potassium carbonate in place of sodium methoxide (as previously published) resulted in moderate improvement. Chlorination of the resulting quinazolone using phosphorus oxychloride in the presence of tetramethylammonium chloride afforded the chloroquinazoline, which was converted in a straightforward manner to the corresponding aminoquinazoline derivatives. Whenever possible, the synthesis was carried out in a parallel format where the reactions were conducted in vials and the products were worked up by parallel solid phase extraction (SPE) using strong cation exchange (SCX) cartridges. Interestingly, attempts to remove the methyl ethers of **38** (in order to install solubilizing functional groups) utilizing boron tribromide caused ring opening of the triazole with concomitant loss of nitrogen, yielding inactive compounds (see SI for details).

All compounds were tested for antibacterial activity against a common laboratory strain of *S. aureus*, RN4220, and against the isogenic RN4220  $\Delta\text{tarO}$  strain, which lacks the first gene in the biosynthetic pathway and is thus not susceptible to WTA inhibitors. This latter strain allows for assessment of compound specificity since any toxic effects against it must be due to mechanisms other than WTA inhibition. The minimum inhibitory concentrations (MIC) of all

compounds are reported against both strains in Tables 1 and 2 and Figure 3. Active compounds were subsequently tested against clinical *S. aureus* isolates (see Table 3).

The first analog library was designed to investigate the positions, sizes and electronics of the A-ring substituents. Commercial starting materials were chosen to probe the amenability of this area of the molecule to derivatization. The chloro group was placed at all possible locations on the A-ring (2–4), but activity was lost when this functionality was displayed anywhere other than C2. Therefore, we sought to optimize the substituent at this position. Modest changes at the C2 position (*i.e.*, F, Me, Br, NO<sub>2</sub>, CN; 5–9) gave compounds with lower activity than the parent C2-chloro compound (1). Replacement of the chloro group with a methyl (6), bromo (7), or methoxy (10) substituent was tolerated, while a fluoro (5), nitro (8), or cyano (9) group abolished activity. From these data, it appears that size rather than electronics is the determining factor for activity. Likewise, substituents displayed at the C3 position resulted in inactive compounds 11–14. Surprisingly, however, 2,3-dimethoxy substitution on the A-ring yielded a potent compound (15). Since both the mono-methoxy derivatives (10 and 14) are less active than the parent compound 1, the effects of changing these positions are not additive. The benzodioxane analog (16) was also prepared, but found to be inactive, suggesting that some flexibility of the substituents may be important. The 2,3-dimethoxy substitution on the A-ring was incorporated into additional analogs in anticipation that it would give improved physicochemical properties (*e.g.*, cLogP) compared to the C2 chloro.

With the A-ring substitution fixed, variations to the amine side chains of the B-ring (Figure 3) were examined, including several primary and secondary amines (17–36), but few variants matched the potency of the parent diethylamine side chain (15). From the MIC data, it was clear that neither a hydrophilic moiety (*e.g.*, 21, 27, 28, 30) nor a larger, hydrophobic group (*e.g.*, 19, 20, 33–36) was tolerated. Only the acyclic secondary amines of small alkyl groups imparted reasonable antibacterial activity (*i.e.*, 24–26). It is surmised that this residue binds to a hydrophobic pocket that is of limited size and depth so that it can only accommodate C<sub>2</sub>–C<sub>4</sub> alkyl groups at the nitrogen atom. Therefore, additional optimization was pursued retaining the diethylamine group on the B-ring.

Finally, we explored changes to the D-ring. Compounds 37 and 38 were made, which contain a *para*-methyl and *para*-chloro substituent on the D-ring, respectively. The 4-chlorophenylsulfone analog (38) exhibited the highest antibacterial activity of all compounds made, with an MIC of 0.3 μM against the *S. aureus* lab strain (RN4220), which shows that modifying the D-ring can have beneficial effects. A broader exploration of D-ring substitutions was hampered by the lack of commercially available arylsulfonyl-acetonitriles. However, since the biological activity of 38 is sufficient (see below) we did not pursue other synthetic approaches to make D-ring analogs. Efforts to combine the best features from each sublibrary (namely, the 2,3-di-OMe on the A-ring, ethylisopropylamine on the B-ring and *para*-chloro on the D-ring) generated 39. However, its activity was not improved over 38.

The original inhibitor 1 and two representative active analogs (15 and 38) were tested against four additional *S. aureus* strains (Table 3). All showed growth inhibitory activities against both methicillin-sensitive (RN6390 and Newman) and methicillin-resistant (MW2 and COL) *S. aureus* strains, with 38 consistently showing the most potent activity.

Compound 38, which we have named targocil, has a bacteriostatic mechanism of action like the original compound (1). Its activity depends on flux into the WTA biosynthetic pathway since the  $\Delta tarO$  mutant is not susceptible (see Table 2). Several lines of evidence indicate that targocil (38) inhibits the same target in the WTA biosynthetic pathway as 1. For example, targocil (38) shows cross-resistance with mutants selected against 1. Some of these characterized mutant strains contain point mutations in *tarG*; others contain mutations in

*tarO* that abolish the expression of WTAs, making the TarG transporter nonessential. Furthermore, resistant mutations selected against targocil (**38**) itself map to *tarG* as well as *tarO*.

One surprising finding was that the measured mutational frequency of *S. aureus* Newman for targocil (**38**) was found to be  $7 \times 10^{-7}$  per cell division, which is at least 10-fold lower than the frequency estimated for compound **1**.<sup>14, 16</sup> The measured frequency of resistance to targocil (**38**) *in vitro* is still higher than is typically desirable, but many of the resistant mutants are pathway nulls. Since these mutants are avirulent, they are not expected to contribute to resistance *in vivo*, and the compound is thus highly promising.<sup>9, 10</sup>

The acute toxicity of targocil (**38**) is acceptable. Doses of 75 mg/kg administered via tail vein injection (see SI for details) caused no adverse effects in mice after 24 h. Although the MIC of targocil (**38**) shifts by a factor of eight in the presence of 50% fetal bovine serum, its tolerated dose in mice is greater than 100-fold the serum MIC.

In conclusion, a structure-activity relationship study of the WTA inhibitor **1** identified positions that are tolerant of substitution and led to the discovery of an analog (targocil, **38**) that is ten-fold more potent than the original screening hit while also having a ten-fold reduced mutational frequency. Targocil (**38**) is active against methicillin-sensitive and resistant clinical strains, and analysis of resistant mutants shows that it inhibits the same target as **1** (TarG). Its properties suggest that it is a candidate for proof of concept studies to address whether inhibiting WTA biosynthesis is a promising strategy for treating bacterial infections *in vivo*.

## Supplementary Material

Refer to Web version on PubMed Central for supplementary material.

## Acknowledgments

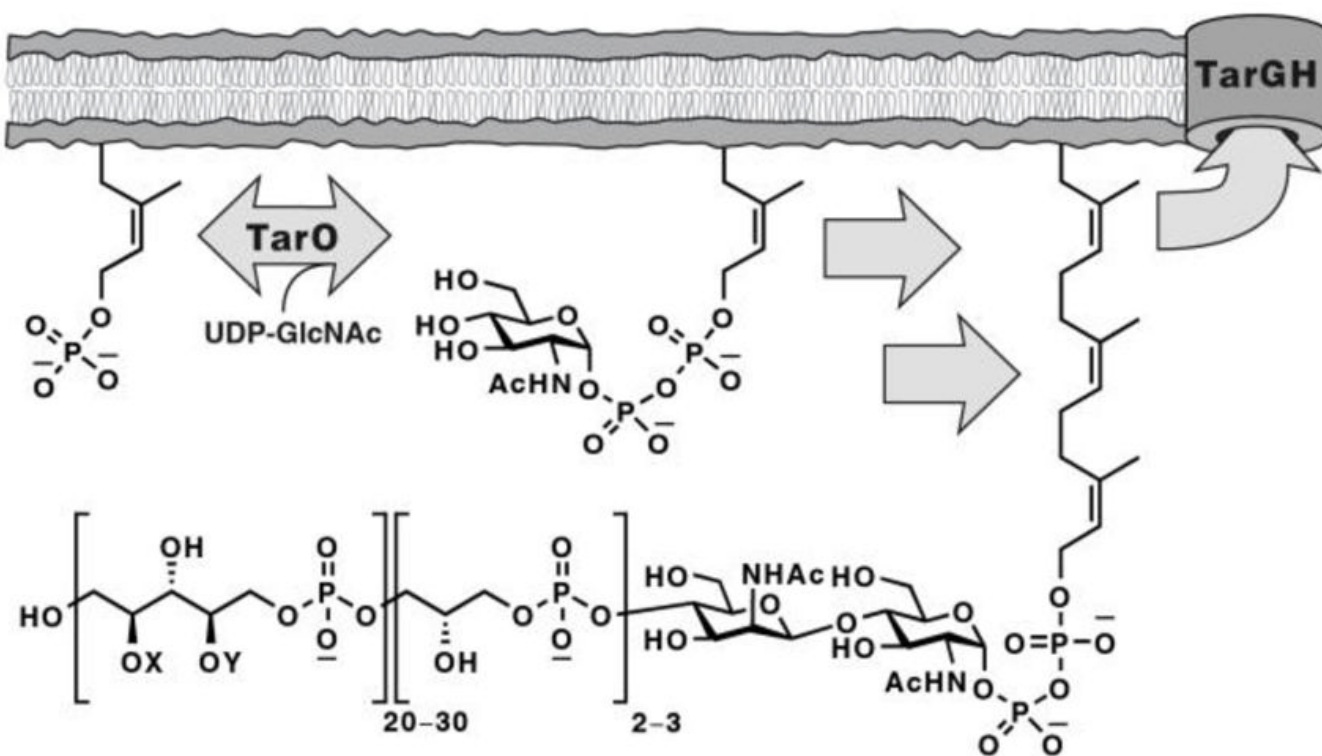
This work was supported by the NIH (1P01AI083214 and 5R01GM078477 to S.W., F32AI084316 to J.C., and F3178727 to J.G.S.) and support to K.L. and G.D.C. was provided by the National Screening Laboratory for the Regional Centers of Excellence in Biodefense and Emerging Infectious Diseases (NIAID U54 AI057159). We would like to thank Su Chiang and Gerald Beltz for helpful discussions.

Supporting data associated with this article can be found, in the online version, at ...

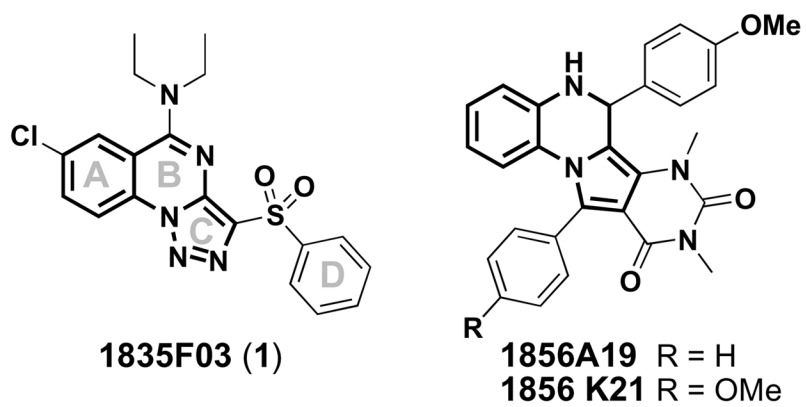
## References

1. Boucher HW, Corey GR. Clin Infect Dis 2008;46(Suppl 5):S344. [PubMed: 18462089]
2. Morbidity and Mortality Weekly Report 2002;51:565. [PubMed: 12139181]
3. Morbidity and Mortality Weekly Report 2002;51:902. [PubMed: 12418544]
4. Morbidity and Mortality Weekly Report 2004;53:322. [PubMed: 15103297]
5. Brickner SJ, Barbachyn MR, Hutchinson DK, Manninen PR. J Med Chem 2008;51:1981. [PubMed: 18338841]
6. Hentschke M, Saager B, Horstkotte MA, Scherpe S, Wolters M, Kabisch H, Grosse R, Heisig P, Aepfelbacher M, Rohde H. Infection 2008;36:85. [PubMed: 18165857]
7. Skiest DJ. J Clin Microbiol 2006;44:655. [PubMed: 16455939]
8. Ratnaraja N, Hawkey PM. Expert Rev Anti Infect Ther 2008;6:601. [PubMed: 18847401]
9. Weidenmaier C, Kokai-Kun J, Kristian S, Chanturiya T, Kalbacher H, Gross M, Nicholson G, Neumeister B, Mond J, Peschel A. Nat Med 2004;10:243. [PubMed: 14758355]
10. Weidenmaier C, Peschel A. Nat Rev Microbiol 2008;6:276. [PubMed: 18327271]
11. Neuhaus F, Baddiley J. Microbiol Mol Biol Rev 2003;67:686. [PubMed: 14665680]
12. Swoboda JG, Campbell J, Meredith TC, Walker S. Chem Bio Chem. 2009 in press.

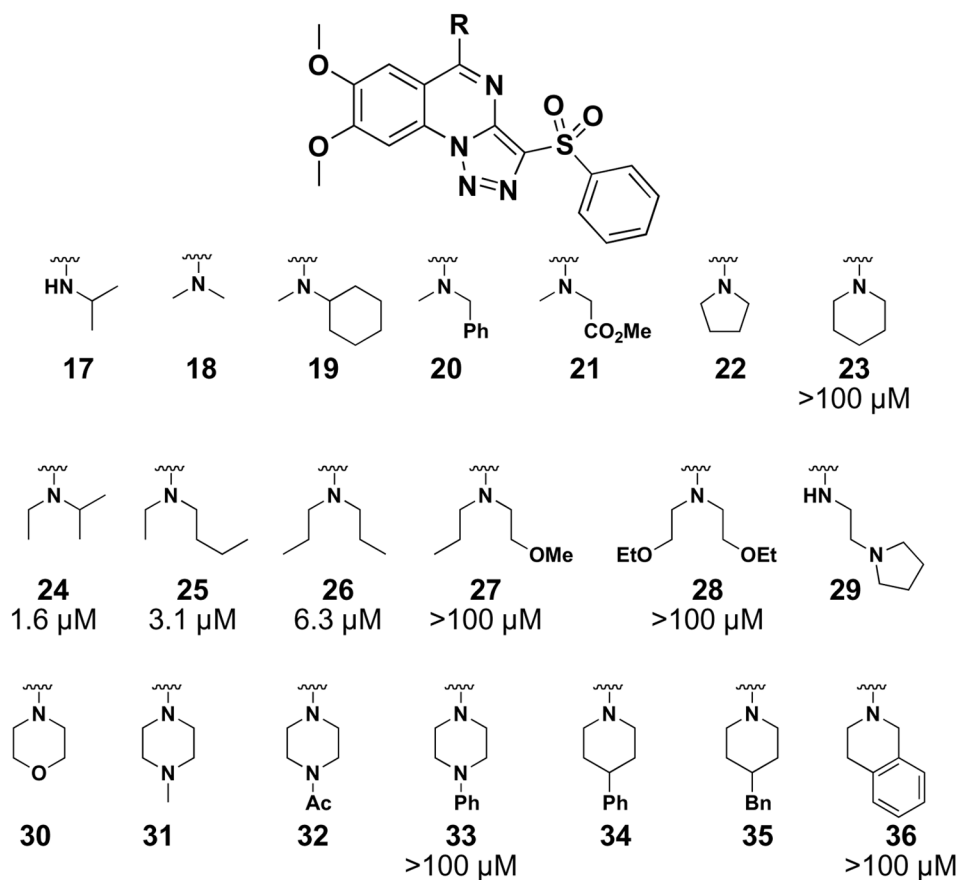
13. D'Elia MA, Pereira MP, Chung YS, Zhao W, Chau A, Kenney TJ, Sulavik MC, Black TA, Brown ED. *J Bacteriol* 2006;188:4183. [PubMed: 16740924]
14. Swoboda JG, Meredith TC, Campbell J, Brown S, Suzuki T, Bollenbach T, Malhowski AJ, Kishony R, Gilmore MS, Walker S. *ACS Chem Biol* 2009;4:875. [PubMed: 19689117]
15. Jones P, Chambers M. *Tetrahedron* 2002;58:9973.
16. Haddix PL, Paulsen ET, Werner TF. *Bioscene* 2000;26:17.



**Figure 1.** Poly(ribitol-phosphate) wall teichoic acids are constructed on a bactoprenol carrier lipid (C<sub>55</sub>~P; partial structures shown here) embedded in the cytoplasmic membrane in *S. aureus*. TarGH is the ABC transporter that exports WTAs and is the target of the class of small molecule antibiotics described here. X and Y denote tailoring modifications of the WTA polymer (e.g., alanylation and glycosylation).

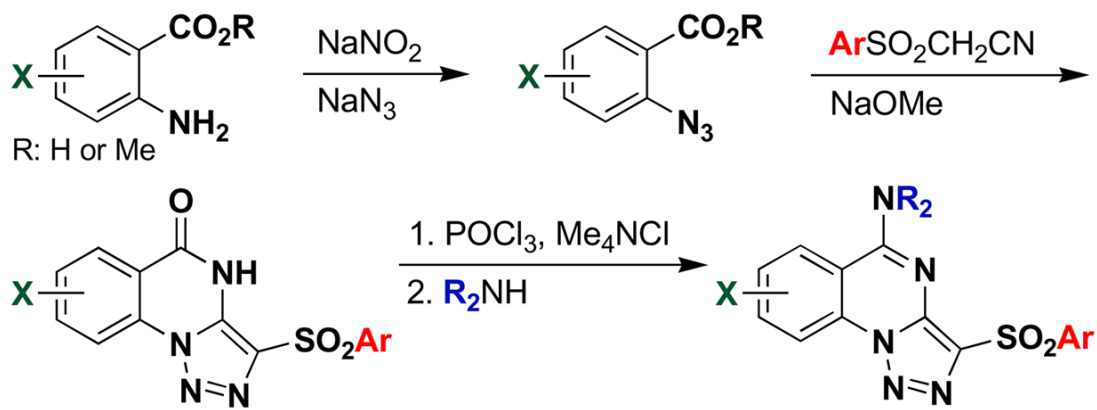


**Figure 2.**  
Chemical structures of the most active hits discovered in our high-throughput screen, with “common” core structures shown in bold.

**Figure 3.**

SAR of the B-ring amine side chains. MICs are given as the lowest concentration of compound (tested) that gave >90% growth inhibition in wildtype *S. aureus* RN4220. MICs are represented as >100  $\mu\text{M}$  if the derivative gave between 31 and 89% growth inhibition at the highest concentration tested (100  $\mu\text{M}$ ). Compounds **33** and **36** showed greater than 70% growth inhibition in the  $\Delta tarO$  mutant at 100  $\mu\text{M}$ , whereas the remaining derivatives gave less than 30% growth inhibition (data not shown).

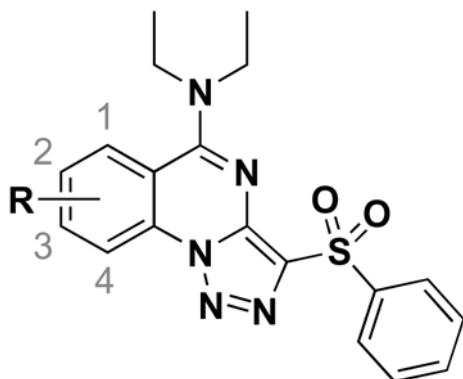




**Scheme 1.**  
Synthesis of triazoloquinazoline analogs.

**Table 1**

A-ring derivatives and their corresponding minimum inhibitory concentrations (MIC) against *Staphylococcus aureus* RN4220.

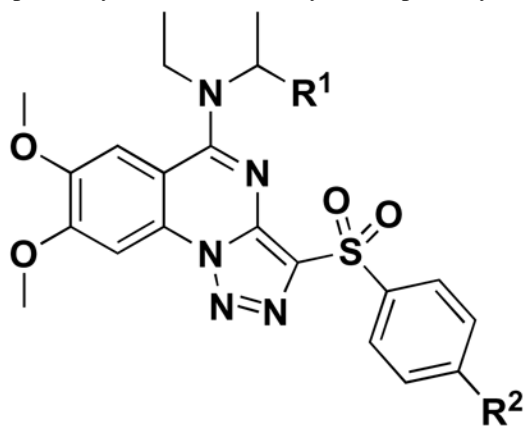


Comps	R	Wildtype <i>S. aureus</i> MIC ( $\mu\text{M}$ )	$\Delta\text{tarO}$ <i>S. aureus</i> MIC ( $\mu\text{M}$ )
1	2-Cl	<b>3.6</b>	na <sup>a</sup>
2	1-Cl	na	na
3	3-Cl	na	na
4	4-Cl	na	na
5	2-F	>100	na
6	2-Me	<b>25</b>	na
7	2-Br	<b>12.5</b>	>100
8	2-NO <sub>2</sub>	>100	na
9	2-CN	na	na
10	2-OMe	<b>25</b>	na
11	3-Me	na	na
12	3-Br	>100	<b>100</b>
13	3-NO <sub>2</sub>	<b>100</b>	<b>50</b>
14	3-OMe	>100	>100
15	2,3-di-OMe	<b>1.8</b>	na
16	2,3-OCH <sub>2</sub> CH <sub>2</sub> O-	na	na

<sup>a</sup> na (not active) indicates <30% growth inhibition at 100  $\mu\text{M}$ . MICs are represented as >100  $\mu\text{M}$  if the compound gave between 31 and 89% growth inhibition at the highest concentration tested (100  $\mu\text{M}$ ).

**Table 2**

D-ring substitutions can enhance biological activity. The lack of activity against the  $\Delta tarO$  strain indicates specificity for the WTA biosynthetic pathway.



Compds	R <sup>1</sup>	R <sup>2</sup>	Wildtype <i>S. aureus</i> MIC (μM)	$\Delta tarO$ <i>S. aureus</i> MIC (μM)
15	H	H	1.8	na <sup>a</sup>
37	H	CH <sub>3</sub>	2.5	na
38	H	Cl	0.3	na
39	CH <sub>3</sub>	Cl	2.5	na

<sup>a</sup> na [not active] indicates <30% growth inhibition at 100 μM.

**Table 3**MICs of the original inhibitor and two analogs against several *S. aureus* strains.

Compds	RN6390 MIC ( $\mu\text{M}$ ) <sup>a</sup>	Newman MIC ( $\mu\text{M}$ )	COL MIC ( $\mu\text{M}$ )	MW2 MIC ( $\mu\text{M}$ )
1	6.3	12.5	6.3	6.3
15	3.1	3.1	3.1	3.1
38	0.3	0.3	0.6	0.6

<sup>a</sup>MICs are given as the lowest concentration of compound (tested) that gave >85% growth inhibition in each strain.